

The effect of temperature-dependent viscosity and thermal conductivity on velocity and temperature field: an analytical solution using the perturbation technique

H. PANAHI-KALUS, M. AHMADINEJAD, A. MOOSAIE^{*)}

*Department of Mechanical Engineering, Yasouj University, 75914-353 Yasouj, Iran,
) e-mail: moosaie@yu.ac.ir (corresponding author)

THIS PAPER PROPOSES A GENERAL FORM OF THE PERTURBATION EXPANSION METHOD for the governing equations of viscous flow coupled to the temperature evolution. The effect of the variations of viscosity and thermal conductivity with temperature on the temperature and velocity fields in a steady two-dimensional Couette–Poiseuille flow is examined. The presented analytical solution by the perturbation method is validated against a finite difference solution of the governing equations. The numerical and analytical solutions are in good agreement.

Key words: temperature-dependent material properties, laminar channel flow, analytical solution, perturbation technique.

Copyright © 2020 by IPPT PAN, Warszawa

1. Introduction

MATERIAL PROPERTIES OF FLUIDS ARE THERMODYNAMIC PROPERTIES, and thus, they generally depend upon the temperature. The temperature dependency of viscosity and thermal conductivity of fluids must be taken into account, if one aims at obtaining more accurate results in thermofluid problems. Although such a thorough analysis may not be of great relevance for water, it is indeed of paramount importance for liquids like industrial lubrication oils and fossil fuels. When the dependence of viscosity upon temperature is considered, the fluid dynamics equations and the heat transfer equation are two-way coupled, i.e. there is a mutual effect of one on the other. Such an interaction phenomenon between the two fields usually complicates the analysis. Moreover, if one considers the dependence of the heat conductivity upon the temperature, the heat equation becomes nonlinear. Both effects hinder the analytical as well as the numerical solution of the problem.

Since the governing equations are often nonlinear in most of the engineering problems, they are of major complexity to be solved analytically. The perturbation method is a well-established technique which is among the prominent methods to analytically approach various kinds of non-linearities. The perturbation technique gives efficient tools to obtain approximate solutions for a wide

range of such problems. This approach is widely used for the problems which do not have a known exact solution, but can be stated as a small change to a solvable problem, see [1] for a general introduction to perturbation methods as used in applied mechanics. A classic book on applications of the perturbation method in fluid mechanics is [2]. A more recent review on applications in fluid mechanics is given in [3].

SAKIADIS [4] was one of the first investigators to study the behavior of boundary-layer flow of a viscous fluid over a moving wall in different perspectives. CRANE [5] has explored an incompressible, two-dimensional, steady boundary-layer flow over a stretching sheet in which the velocity linearly changes with the distance from a stationary point. KAFOUSSIAS *et al.* [6] have studied the influence of temperature dependence of viscosity on an incompressible fluid in steady laminar mixed convective boundary layer over an isothermal flat plate. They have solved the coupled ordinary differential equations with a numerical technique. XENOS [7] has reported the radiation effects on flow past a stretching plate with temperature-dependent viscosity. Numerous investigations have considered the effects of temperature-dependent thermal conductivity and viscosity properties in fluid. The effect of temperature dependence of viscosity on the heat transfer over a steadily moving surface has been explored by ELBASHBESHY *et al.* [8]. The vital features of heat transfer in an electrically conducting fluid with heat generation and temperature-dependent viscosity have been investigated by PAL and MONDAL [9]. Solutions for two stagnation flows of an incompressible Newtonian fluid with exponentially temperature-dependent viscosity have been derived by EMERMAN *et al.* [10]. PEARSON [11] has presented a similarity solution for a two-dimensional flow in a channel whose viscosity varies exponentially with temperature. The similarity transformation has been used to reduce the time-independent boundary-layer equations into coupled ordinary differential equations in order to examine the effects of temperature-dependent viscosity and thermal conductivity on the flow and heat transfer over a horizontal shrinking sheet by KHAN *et al.* [12].

BOOKER [13] has experimentally investigated the heat transfer and the structure of convection in a high Prandtl number fluid layer whose viscosity is variable with temperature. They have transformed the boundary-layer equations to ordinary differential equations including a viscosity/temperature parameter and the Prandtl number. GIUDICE *et al.* [14] have performed a numerical study considering a linear variation of viscosity with respect to temperature and examined the effects of viscous dissipation in laminar flows through microchannels. HOSAIN *et al.* [15] have considered a forced flow and heat transfer of a viscous incompressible fluid in which viscosity and thermal conductivity vary with temperature using appropriate transformations to reduce the governing equations to non-similarity equations. ATTIA [16] has studied the effects of temperature-

dependent viscosity and heat transfer on the Couette flow of a dusty fluid between two parallel plates with a uniform magnetic field which influences the flow in the direction perpendicular to the walls. YUAN *et al.* [17] have developed a method for predicting the temperature-dependent viscosity of biodiesel based on fatty acid ester compositions. AVELLANEDA *et al.* [18] have performed a direct numerical simulation (DNS) for a fully-developed low Mach turbulent flow of an ideal gas in which the variation of viscosity and thermal conductivity are assumed to be as presented by SUTHERLAND [19].

Using analytical tools, ELLAHI [20] has investigated the effects of various physical parameters on velocity, temperature and nano-particle concentration in a pipe by considering two correlations for the temperature-dependent viscosity. VERGORI [21] has probed the flows of fluids whose material properties vary analytically with temperature and pressure at small Reynolds and Froude numbers in a horizontal channel. CHAIM [22] has discussed the mathematical model of two-dimensional axisymmetric fluid flows along a continuously stretching sheet in which variable thermal conductivity and viscous dissipation are taken into account.

Perturbation techniques are often used in order to solve non-linear equations analytically. This method has always been a practical way for many researchers and has been utilized in numerous works. LIN *et al.* [23] have considered two approaches to investigate the effect of temperature-dependent viscosity, a known exponential function expressing the temperature-viscosity relation and using the perturbation technique for small heat transfer rates. Their perturbation results are in excellent agreement with those of the direct method. DEGHAN *et al.* [24] have analytically analyzed the impacts of temperature-dependent thermal conductivity in a plane channel flow of a fluid-saturated porous medium based on the perturbation methods. They have presented analytical relations for dimensionless temperature profile and the Nusselt number for the first time. Their work shows that there is a linear relation between thermal conductivity and the Nusselt number. MOOSAIE [25] has proposed an analytical solution of thermal stresses in a hollow cylinder with variable temperature-dependent material properties using the perturbation technique to solve the non-linear heat conduction equation. MOOSAIE and PANAHI-KALUS [26] have used the perturbation technique to analyze a non-linear static thermoelastic analysis of a hollow spherical shell.

The main objective of the present work is to propose a general and novel form of the perturbation technique in the symbolic form for conservation laws of mass, momentum and energy. Moreover, the proposed form of conservation equations is in the general tensor notation, independent of the coordinate system applied. The temperature dependence of viscosity and thermal conductivity are taken into account as well. The variations of viscosity and thermal conductivity

with temperature are assumed to be linear. To the best of our knowledge, so far this general form of the perturbation technique has not been yet presented elsewhere. To put the work into a practical use, a numerical example of a channel flow has been solved analytically for prescribed boundary conditions. In order to validate the present study, the analytical solution has been compared to the numerical one.

2. Theory and governing equations

Let us first consider the conservation laws including incompressible form of continuity, momentum and energy equations in the differential form. Note that \mathbf{u} is the velocity and T is the temperature.

$$(2.1) \quad \nabla \cdot \mathbf{u} = 0,$$

$$(2.2) \quad \rho \left(\frac{\partial \mathbf{u}}{\partial t} + (\mathbf{u} \cdot \nabla) \mathbf{u} \right) = \nabla \cdot \mathbf{S} + \mathbf{k},$$

$$(2.3) \quad \rho c \left(\frac{\partial T}{\partial t} + (\mathbf{u} \cdot \nabla) T \right) = \nabla \cdot (\lambda \nabla T) + \dot{q},$$

where ∇ , ρ , c , \mathbf{k} , λ and \dot{q} are the nabla operator, density and specific heat, external force, thermal conductivity and source term, respectively. The viscous dissipation term is neglected in Eq. (2.3), which is a common practice for low-speed incompressible flows. The stress tensor \mathbf{S} for Newtonian fluids can be written as

$$(2.4) \quad \mathbf{S} = -p\mathbf{E} + \mu(\nabla \circ \mathbf{u} + \mathbf{u} \circ \nabla),$$

in which μ is the dynamic viscosity and p is the pressure. In this work, μ is assumed to depend upon the temperature, i.e. $\mu = \mu(T)$. Therefore, the first term in the right-hand side of Eq. (2.2) can be expressed as

$$(2.5) \quad \nabla \cdot \mathbf{S} = -\nabla p + \frac{d\mu}{dT} [(\nabla T \cdot \nabla) \mathbf{u} + \nabla(\nabla T \cdot \mathbf{u})] + \mu \Delta \mathbf{u}.$$

Substituting Eq. (2.5) into Eq. (2.2) yields

$$(2.6a) \quad \rho \left(\frac{\partial \mathbf{u}}{\partial t} + (\mathbf{u} \cdot \nabla) \mathbf{u} \right) = -\nabla p + \frac{d\mu}{dT} [(\nabla T \cdot \nabla) \mathbf{u} + \nabla(\nabla T \cdot \mathbf{u})] + \mu \Delta \mathbf{u} + \mathbf{k},$$

$$(2.6b) \quad \rho c_p \left(\frac{\partial T}{\partial t} + (\mathbf{u} \cdot \nabla) T \right) = \frac{d\lambda}{dT} \nabla T \cdot \nabla T + \lambda \Delta T + \dot{q}.$$

The above equations are coupled together. The variations of viscosity and thermal conductivity are assumed to be linear functions of temperature [27]:

$$(2.7) \quad \begin{cases} \mu = \mu_0 - \mu_1 T; & \mu_0 \gg T_{\text{ref}} \mu_1, \\ \lambda = \lambda_0 + \lambda_1 T; & \lambda_0 \gg T_{\text{ref}} \lambda_1, \end{cases}$$

in which T_{ref} is a reference temperature. Since $T_{\text{ref}}\mu_1$ and $T_{\text{ref}}\lambda_1$ are small compared to μ_0 and λ_0 for some conventional fluids such as water, we can define the following relations

$$(2.8) \quad \varepsilon = \frac{T_{\text{ref}}\mu_1}{\mu_0}, \quad \varepsilon_1 = \frac{T_{\text{ref}}\lambda_1}{\lambda_0}.$$

Without any loss of generality, hereafter T_{ref} is assumed to be unity. Therefore, it will no more appear in the equations.

Using Eq. (2.7) and dividing by μ_0 and λ_0 , the Navier–Stokes is

$$(2.9a) \quad \nabla \cdot \mathbf{u} = 0,$$

$$(2.9b) \quad \frac{\rho}{\mu_0} \left(\frac{\partial \mathbf{u}}{\partial t} + (\mathbf{u} \cdot \nabla) \mathbf{u} \right) = -\nabla p - \varepsilon [(\nabla T \cdot \nabla) \mathbf{u} + \nabla(\nabla T \cdot \mathbf{u})] + (1 - \varepsilon T) \Delta \mathbf{u} + \frac{\mathbf{k}}{\mu_0},$$

$$(2.9c) \quad \frac{\rho c_p}{\lambda_0} \left(\frac{\partial T}{\partial t} + (\mathbf{u} \cdot \nabla) T \right) = \varepsilon_1 \nabla T \cdot \nabla T + (1 + \varepsilon_1 T) \Delta T + \frac{\dot{q}}{\lambda_0}.$$

The ratio of two small parameters ε and ε_1 can be defined by β via

$$(2.10) \quad \beta = \frac{\varepsilon_1}{\varepsilon}.$$

In the above governing equation, we have two dimensionless small parameters ε and ε_1 , which are multiplied to some nonlinear terms. Thus, it makes sense to use the Poincare perturbation method to find an approximate analytical solution of the problem. The method is based on an asymptotic power series expansion of the dependent variables in terms of the small parameters, as done below. Then, various orders of approximations are collected and linear differential equations for different levels of approximation are found. The inhomogeneous boundary conditions are enforced at the zeroth-order approximation and the rest of the boundary-value problems are solved using homogeneous boundary conditions. The details of the mathematical theory and applications in various fields of engineering can be found in [1, 2].

So, the velocity and temperature fields can be expanded as power series of ε , that is

$$(2.11) \quad \mathbf{u} = \sum_{n=0}^{\infty} \varepsilon^n \bar{\mathbf{u}}_n,$$

$$(2.12) \quad T = \sum_{n=0}^{\infty} (\beta \varepsilon)^n \bar{T}_n.$$

These expansions can be truncated at any order to give approximations of velocity and temperature fields. The above equations up to the second-order approximation read

$$(2.13) \quad u_0 = \bar{u}_0, \quad u_1 = \bar{u}_0 + \varepsilon \bar{u}_1, \quad u_2 = \bar{u}_0 + \varepsilon \bar{u}_1 + \varepsilon^2 \bar{u}_2,$$

and

$$(2.14) \quad T_0 = \bar{T}_0, \quad T_1 = \bar{T}_0 + \beta \varepsilon \bar{T}_1, \quad T_2 = \bar{T}_0 + \beta \varepsilon \bar{T}_1 + \beta^2 \varepsilon^2 \bar{T}_2.$$

Substituting Eqs. (2.11) and (2.12) into Eq. (2.9) results in

$$(2.15a) \quad \sum_{n=0}^{\infty} \varepsilon^n \nabla \cdot \bar{\mathbf{u}}_n = 0,$$

$$(2.15b) \quad \begin{aligned} & \frac{\rho}{\mu_0} \left\{ \sum_{n=0}^{\infty} \varepsilon^n \frac{\partial \bar{\mathbf{u}}_n}{\partial t} + \left[\left(\sum_{n=0}^{\infty} \varepsilon^n \bar{\mathbf{u}}_n \right) \cdot \nabla \right] \sum_{n=0}^{\infty} \varepsilon^n \bar{\mathbf{u}}_n \right\} \\ &= -\frac{1}{\mu_0} \nabla p - \left\{ \left[\left(\sum_{n=0}^{\infty} (\beta \varepsilon)^n \bar{T}_n \right) \cdot \nabla \right] \sum_{n=0}^{\infty} \varepsilon^{n+1} \bar{\mathbf{u}}_n \right. \\ & \quad \left. + \nabla \left[\left(\sum_{n=0}^{\infty} (\beta \varepsilon)^n \nabla \bar{T}_n \right) \cdot \sum_{n=0}^{\infty} \varepsilon^{n+1} \bar{\mathbf{u}}_n \right] \right\} \\ & \quad + \left(\sum_{n=0}^{\infty} \varepsilon^n \Delta \bar{\mathbf{u}}_n - \sum_{n=0}^{\infty} (\beta \varepsilon)^n \bar{T}_n \sum_{n=0}^{\infty} \varepsilon^{n+1} \Delta \bar{\mathbf{u}}_n \right) + \frac{\mathbf{k}}{\mu_0}, \end{aligned}$$

$$(2.15c) \quad \begin{aligned} & \frac{\rho c_p}{\lambda_0} \left\{ \sum_{n=0}^{\infty} (\beta \varepsilon)^n \frac{\partial \bar{T}_n}{\partial t} + \left[\left(\sum_{n=0}^{\infty} \varepsilon^n \bar{\mathbf{u}}_n \right) \cdot \nabla \right] \sum_{n=0}^{\infty} (\beta \varepsilon)^n \bar{T}_n \right\} \\ &= \left(\sum_{n=0}^{\infty} (\beta \varepsilon)^{n+1} \nabla \bar{T}_n \right) \cdot \left(\sum_{n=0}^{\infty} (\beta \varepsilon)^n \nabla \bar{T}_n \right) \\ & \quad + \left(1 + \sum_{n=0}^{\infty} (\beta \varepsilon)^{n+1} \bar{T}_n \right) \sum_{n=0}^{\infty} (\beta \varepsilon)^n \Delta \bar{T}_n + \frac{\dot{q}}{\lambda_0}. \end{aligned}$$

By collecting coefficients of like powers of ε^0 , the $O(\varepsilon^0)$ equation is obtained

$$(2.16a) \quad \nabla \cdot \bar{\mathbf{u}}_0 = 0,$$

$$(2.16b) \quad \frac{\rho}{\mu_0} \left[\frac{\partial \bar{\mathbf{u}}_0}{\partial t} + (\bar{\mathbf{u}}_0 \cdot \nabla) \bar{\mathbf{u}}_0 \right] = -\frac{1}{\mu_0} \nabla p + \Delta \bar{\mathbf{u}}_0 + \frac{\mathbf{k}}{\mu_0},$$

$$(2.16c) \quad \frac{\rho c_p}{\lambda_0} \left[\frac{\partial \bar{T}_0}{\partial t} + (\bar{\mathbf{u}}_0 \cdot \nabla) \bar{T}_0 \right] = \Delta \bar{T}_0 + \frac{\dot{q}}{\lambda_0}.$$

Similarly, the $O(\varepsilon^1)$ equations read

$$(2.17a) \quad \nabla \cdot \bar{\mathbf{u}}_1 = 0,$$

$$(2.17b) \quad \frac{\rho}{\mu_0} \left[\frac{\partial \bar{\mathbf{u}}_1}{\partial t} + (\bar{\mathbf{u}}_1 \cdot \nabla) \bar{\mathbf{u}}_0 + (\bar{\mathbf{u}}_0 \cdot \nabla) \bar{\mathbf{u}}_1 \right] \\ = -(\nabla \bar{T}_0 \cdot \nabla) \bar{\mathbf{u}}_0 - \nabla(\nabla \bar{T}_0 \cdot \bar{\mathbf{u}}_0) + \Delta \bar{\mathbf{u}}_1 - \bar{T}_0 \Delta \bar{\mathbf{u}}_0,$$

$$(2.17c) \quad \frac{\rho c_p}{\lambda_0} \left[\frac{\partial \bar{T}_1}{\partial t} + (\bar{\mathbf{u}}_1 \cdot \nabla) \bar{T}_0 + (\bar{\mathbf{u}}_0 \cdot \nabla) \beta \bar{T}_1 \right] \\ = +\beta \nabla \bar{T}_0 \cdot \nabla \bar{T}_0 + \beta \Delta \bar{T}_1 + \beta \bar{T}_0 \Delta \bar{T}_0.$$

Finally, the $O(\varepsilon^2)$ equations are

$$(2.18a) \quad \nabla \cdot \bar{\mathbf{u}}_2 = 0,$$

$$(2.18b) \quad \frac{\rho}{\mu_0} \left[\frac{\partial \bar{\mathbf{u}}_2}{\partial t} + (\bar{\mathbf{u}}_2 \cdot \nabla) \bar{\mathbf{u}}_0 + (\bar{\mathbf{u}}_0 \cdot \nabla) \bar{\mathbf{u}}_2 + (\bar{\mathbf{u}}_1 \cdot \nabla) \bar{\mathbf{u}}_1 \right] \\ = -(\beta \nabla \bar{T}_1 \cdot \nabla) \bar{\mathbf{u}}_0 - (\nabla \bar{T}_0 \cdot \nabla) \bar{\mathbf{u}}_1 \\ - \nabla(\beta \nabla \bar{T}_1 \cdot \bar{\mathbf{u}}_0) - \nabla(\nabla \bar{T}_0 \cdot \bar{\mathbf{u}}_1) + \Delta \bar{\mathbf{u}}_2 - \beta \bar{T}_1 \Delta \bar{\mathbf{u}}_0 - \bar{T}_0 \Delta \bar{\mathbf{u}}_1,$$

$$(2.18c) \quad \frac{\rho c_p}{\lambda_0} \left[\frac{\partial \bar{T}_2}{\partial t} + (\bar{\mathbf{u}}_2 \cdot \nabla) \bar{T}_0 + (\bar{\mathbf{u}}_1 \cdot \nabla) \beta \bar{T}_1 + (\bar{\mathbf{u}}_0 \cdot \nabla) \beta^2 \bar{T}_2 \right] \\ = \beta^2 \nabla \bar{T}_1 \cdot \nabla \bar{T}_0 + \beta^2 \nabla \bar{T}_0 \cdot \nabla \bar{T}_1 + \beta^2 \Delta \bar{T}_2 + \beta^2 \bar{T}_1 \Delta \bar{T}_0 + \beta^2 \bar{T}_0 \Delta \bar{T}_1.$$

It shall be noted here that the zeroth-order equations correspond to the case for which the viscosity and thermal conductivity are constant. Once they are obtained, the zeroth-order results are substituted into the right-hand side of the first-order equations. Again, by solving for the first-order solution, the results are given to the right-hand side of the second-order equations. Theoretically, this procedure can be continued up to any order.

The equations presented in this section are derived in the general tensor form, which can be transformed into different coordinate systems and various geometries. These series can be continued and more terms could be retained. However, in this paper, we have restricted ourselves to the above order of approximation and do not go any further.

3. Case study

In order to put the present perturbation technique into a practical use, a numerical example is demonstrated. The problem which is considered here is a two-dimensional Couette–Poiseuille flow with prescribed boundary conditions as follows:

$$(3.1) \quad \begin{cases} u(y=0) = \bar{u}_l, \\ u(y=H) = \bar{u}_d, \\ T(y=0) = \bar{T}_l, \\ T(y=H) = \bar{T}_d, \end{cases}$$

in which \bar{u} and \bar{T} are respectively the prescribed velocities and temperatures at the boundary. l and d indices imply lower and upper walls. The non-homogeneities of the boundary conditions are given to the zeroth-order approximation and the boundary conditions for the higher-order approximations are homogeneous.

The derived general Eqs. (2.16), (2.17) and (2.18) are rewritten into the Cartesian coordinate system for the considered problem. We assume the flow problem to be steady-state, two-dimensional, fully-developed in the flow direction, with no source term and the external forces are assumed negligible as well.

By casting the $O(\varepsilon^0)$ momentum equation (2.16b) and energy equation (2.16c), we have

$$(3.2a) \quad \frac{\rho}{\mu_0} \left(\bar{u}_0 \frac{\partial \bar{u}_0}{\partial x} + \bar{v}_0 \frac{\partial \bar{v}_0}{\partial y} \right) = -\frac{1}{\mu_0} \frac{\partial P}{\partial x} + \left(\frac{\partial^2 \bar{u}_0}{\partial x^2} + \frac{\partial^2 \bar{u}_0}{\partial y^2} \right),$$

$$(3.2b) \quad \frac{\rho c_p}{\lambda_0} \left(\bar{u}_0 \frac{\partial \bar{T}_0}{\partial x} + \bar{v}_0 \frac{\partial \bar{T}_0}{\partial y} \right) = \frac{\partial^2 \bar{T}_0}{\partial x^2} + \frac{\partial^2 \bar{T}_0}{\partial y^2}.$$

By imposing the aforementioned assumptions, we have

$$(3.3a) \quad \frac{\partial^2 \bar{u}_0}{\partial y^2} = \frac{1}{\mu_0} \frac{\partial P}{\partial x} = A,$$

$$(3.3b) \quad \frac{\partial^2 \bar{T}_0}{\partial y^2} = 0,$$

so that the zeroth-order solution read

$$(3.4a) \quad \bar{u}_0(y) = \frac{1}{2}Ay^2 + C_{1,0}y + C_{2,0},$$

$$(3.4b) \quad \bar{T}_0(y) = D_{1,0}y + D_{2,0}.$$

Now the general solution of $O(\varepsilon^0)$ is subjected to homogeneous boundary conditions.

Applying the above boundary conditions to Eqs. (3.4) gives the integration constants as

$$(3.5) \quad C_{1,0} = \frac{\bar{u}_d - \bar{u}_l}{H} - \frac{A}{2}H, \quad C_{2,0} = \bar{u}_l, \quad D_{1,0} = \frac{\bar{T}_d - \bar{T}_l}{H}, \quad D_{2,0} = \bar{T}_l.$$

By casting the $O(\varepsilon^1)$ momentum equation (2.17b) and energy equation (2.17c) is

$$(3.6a) \quad \frac{\rho}{\mu_0} \left(\bar{u}_1 \frac{\partial \bar{u}_0}{\partial x} + \bar{v}_1 \frac{\partial \bar{v}_0}{\partial y} + \bar{u}_0 \frac{\partial \bar{u}_1}{\partial x} + \bar{v}_0 \frac{\partial \bar{v}_1}{\partial y} \right) \\ = - \frac{\partial \bar{T}_0}{\partial x} \frac{\partial \bar{u}_0}{\partial x} - \frac{\partial \bar{T}_0}{\partial y} \frac{\partial \bar{u}_0}{\partial y} - \frac{\partial \bar{T}_0}{\partial x} \frac{\partial \bar{u}_0}{\partial x} \\ - \frac{\partial \bar{T}_0}{\partial y} \frac{\partial \bar{v}_0}{\partial x} + \left(\frac{\partial^2 \bar{u}_1}{\partial x^2} + \frac{\partial^2 \bar{u}_1}{\partial y^2} \right) - \bar{T}_0 \frac{\partial^2 \bar{u}_0}{\partial y^2},$$

$$(3.6b) \quad \frac{\rho c_p}{\lambda_0} \left(\bar{u}_1 \frac{\partial \bar{T}_0}{\partial x} + \bar{v}_1 \frac{\partial \bar{T}_0}{\partial y} + \beta \bar{u}_0 \frac{\partial \bar{T}_1}{\partial x} + \beta \bar{v}_0 \frac{\partial \bar{T}_1}{\partial y} \right) \\ = -\beta \left[\left(\frac{\partial \bar{T}_0}{\partial x} \right)^2 + \left(\frac{\partial \bar{T}_0}{\partial y} \right)^2 \right] + \beta \left(\frac{\partial^2 \bar{T}_1}{\partial x^2} + \frac{\partial^2 \bar{T}_1}{\partial y^2} \right) - \beta \bar{T}_0 \frac{\partial^2 \bar{T}_0}{\partial y^2}.$$

Imposing the assumptions, we have

$$(3.7a) \quad \frac{\partial^2 \bar{u}_1}{\partial y^2} = \frac{\partial \bar{T}_0}{\partial y} \frac{\partial \bar{u}_0}{\partial y} + \bar{T}_0 \frac{\partial^2 \bar{u}_0}{\partial y^2},$$

$$(3.7b) \quad \frac{\partial^2 \bar{T}_1}{\partial y^2} = - \left(\frac{\partial \bar{T}_0}{\partial y} \right)^2 - \bar{T}_0 \frac{\partial^2 \bar{T}_0}{\partial y^2}.$$

Solving these equations gives

$$(3.8a) \quad \bar{u}_1(y) = \frac{1}{3} D_{1,0} A y^3 + \frac{1}{2} (C_{1,0} D_{1,0} + A D_{2,0}) y^2 + C_{1,1} y + C_{2,1},$$

$$(3.8b) \quad \bar{T}_1(y) = -\frac{1}{2} D_{1,0}^2 y^2 + D_{1,1} y + D_{2,1}.$$

The boundary conditions for the $O(\varepsilon^1)$ equations are homogeneous.

The integration constants are determined by applying the boundary conditions as

$$(3.9) \quad C_{1,1} = -\frac{1}{3} A D_{1,0} H^2 - \frac{1}{2} (C_{1,0} D_{1,0} + A D_{2,0}) H, \\ C_{2,1} = 0, \quad D_{1,1} = \frac{1}{2} D_{1,0}^2 H, \quad D_{2,1} = 0.$$

Finally, the expansion of $O(\varepsilon^2)$ for momentum equation (2.18b) and energy equation (2.18c) is

$$\begin{aligned}
(3.10a) \quad & \frac{\rho}{\mu_0} \left(\bar{u}_2 \frac{\partial \bar{u}_0}{\partial x} + \bar{v}_2 \frac{\partial \bar{v}_0}{\partial y} + \bar{u}_1 \frac{\partial \bar{u}_1}{\partial x} + \bar{v}_1 \frac{\partial \bar{v}_1}{\partial y} + \bar{u}_0 \frac{\partial \bar{u}_2}{\partial x} + \bar{v}_0 \frac{\partial \bar{v}_2}{\partial y} \right) \\
& = -\beta \frac{\partial \bar{T}_1}{\partial x} \frac{\partial \bar{u}_0}{\partial x} - \frac{\partial \bar{T}_0}{\partial x} \frac{\partial \bar{u}_1}{\partial x} - \beta \frac{\partial \bar{T}_1}{\partial y} \frac{\partial \bar{u}_0}{\partial y} - \frac{\partial \bar{T}_0}{\partial y} \frac{\partial \bar{u}_1}{\partial y} \\
& \quad - \beta \frac{\partial \bar{T}_1}{\partial x} \frac{\partial \bar{u}_0}{\partial x} - \beta \frac{\partial \bar{T}_1}{\partial y} \frac{\partial \bar{v}_0}{\partial x} - \frac{\partial \bar{T}_0}{\partial x} \frac{\partial \bar{u}_1}{\partial x} - \frac{\partial \bar{T}_0}{\partial y} \frac{\partial \bar{v}_1}{\partial x} + \frac{\partial^2 \bar{u}_2}{\partial x^2} \\
& \quad + \frac{\partial^2 \bar{u}_2}{\partial y^2} - \beta \bar{T}_1 \frac{\partial^2 \bar{u}_0}{\partial y^2} - \bar{T}_0 \frac{\partial^2 \bar{u}_1}{\partial y^2},
\end{aligned}$$

$$\begin{aligned}
(3.10b) \quad & \frac{\rho c_p}{\lambda_0} \left(\bar{u}_2 \frac{\partial \bar{T}_0}{\partial x} + \bar{v}_2 \frac{\partial \bar{T}_0}{\partial y} + \beta \bar{u}_1 \frac{\partial \bar{T}_1}{\partial x} + \beta \bar{v}_1 \frac{\partial \bar{T}_1}{\partial y} + \beta^2 \bar{u}_0 \frac{\partial \bar{T}_2}{\partial x} + \beta^2 \bar{v}_0 \frac{\partial \bar{T}_2}{\partial y} \right) \\
& = \beta^2 \left(\frac{\partial^2 \bar{T}_2}{\partial x^2} + \frac{\partial^2 \bar{T}_2}{\partial y^2} \right) + \beta^2 \left[\frac{\partial \bar{T}_1}{\partial x} \frac{\partial \bar{T}_0}{\partial x} + \frac{\partial \bar{T}_1}{\partial y} \frac{\partial \bar{T}_0}{\partial y} \right] \\
& \quad + \beta^2 \left[\frac{\partial \bar{T}_0}{\partial x} \frac{\partial \bar{T}_1}{\partial x} + \frac{\partial \bar{T}_0}{\partial y} \frac{\partial \bar{T}_1}{\partial y} \right] + \beta^2 \bar{T}_1 \frac{\partial^2 \bar{T}_0}{\partial y^2} \\
& \quad + \beta^2 \bar{T}_0 \left[\left(\frac{\partial \bar{T}_0}{\partial x} \right)^2 + \left(\frac{\partial \bar{T}_0}{\partial y} \right)^2 \right].
\end{aligned}$$

By applying the above-mentioned assumptions, we have

$$(3.11a) \quad \frac{\partial^2 \bar{u}_2}{\partial y^2} = \beta \frac{\partial \bar{T}_1}{\partial y} \frac{\partial \bar{u}_0}{\partial y} + \frac{\partial \bar{T}_0}{\partial y} \frac{\partial \bar{u}_1}{\partial y} + \beta \bar{T}_1 \frac{\partial^2 \bar{u}_0}{\partial y^2} + \bar{T}_0 \frac{\partial^2 \bar{u}_1}{\partial y^2},$$

$$(3.11b) \quad \frac{\partial^2 \bar{T}_2}{\partial y^2} = -2 \frac{\partial \bar{T}_1}{\partial y} \frac{\partial \bar{T}_0}{\partial y} - \bar{T}_1 \frac{\partial^2 \bar{T}_0}{\partial y^2} - \bar{T}_0 \left(\frac{\partial \bar{T}_0}{\partial y} \right)^2,$$

with the general solution

$$(3.12a) \quad \bar{u}_2(y) = \frac{1}{12} \gamma y^4 + \frac{1}{6} \Gamma y^3 + \frac{1}{2} \xi y^2 + C_{1,2} y + C_{2,2},$$

$$(3.12b) \quad \bar{T}_2(y) = \frac{1}{6} D_{1,0}^3 y^3 - \frac{1}{2} (2D_{1,0} D_{1,1} + D_{1,0}^2 D_{2,0}) y^2 + D_{1,2} y + D_{2,2}.$$

The boundary conditions for the $O(\varepsilon^2)$ equations are also homogeneous, which yield the following integration constants

$$C_{1,2} = -\frac{1}{12} \gamma H^3 - \frac{1}{6} \Gamma H^2 - \frac{1}{2} \xi H, \quad C_{2,2} = 0,$$

$$D_{1,2} = -\frac{1}{6} D_{1,0}^3 H^2 + \frac{1}{2} (2D_{1,0} D_{1,1} + D_{1,0}^2 D_{2,0}) H, \quad D_{2,2} = 0.$$

For the convenience, the auxiliary parameters γ , Γ and ξ are defined as

$$\begin{aligned} \gamma &= -A\beta D_{1,0}^2 + AD_{1,0}^2 - \frac{1}{2}A\beta D_{1,0}^2 + 2AD_{1,0}^2, \\ \Gamma &= 2A\beta D_{1,1} - \beta C_{1,0}D_{1,0}^2 + 2C_{1,0}D_{1,0}^2 + 4AD_{1,0}D_{2,0}, \\ \xi &= \beta C_{1,0}D_{1,1} + C_{1,1}D_{1,0} + A\beta D_{2,1} + AD_{2,0}^2 + C_{1,0}D_{1,0}D_{2,0}. \end{aligned}$$

The velocity and temperature fields are calculated for different orders of ε to give the following approximations up to $O(\varepsilon^2)$:

$$\begin{aligned} (3.13a) \quad u_2(y) &= \varepsilon^0 \left(\frac{1}{2}Ay^2 + C_{1,0}y + C_{2,0} \right) \\ &+ \varepsilon^1 \left[\frac{1}{3}D_{1,0}Ay^3 + \frac{1}{2}(C_{1,0}D_{1,0} + AD_{2,0})y^2 + C_{1,1}y + C_{2,1} \right] \\ &+ \varepsilon^2 \left(\frac{1}{12}\gamma y^4 + \frac{1}{6}\Gamma y^3 + \frac{1}{2}\xi y^2 + C_{1,2}y + C_{2,2} \right), \end{aligned}$$

$$\begin{aligned} (3.13b) \quad T_2(y) &= \varepsilon^0(D_{1,0}y + D_{2,0}) + \varepsilon^1 \left(-\frac{1}{2}D_{1,0}^2y^2 + D_{1,1}y + D_{2,1} \right) \\ &+ \varepsilon^2 \left[\frac{1}{6}D_{1,0}^3y^3 - \frac{1}{2}(2D_{1,0}D_{1,1} + D_{1,0}^2D_{2,0})y^2 + D_{1,2}y + D_{2,2} \right]. \end{aligned}$$

4. Numerical solution of the case study

The full nonlinear equations for fluid flow and heat transfer, i.e. Eqs. (2.9b) and (2.9c), for the above-referenced case study reduce to

$$(4.1) \quad (1 - \varepsilon T) \frac{\partial^2 u}{\partial y^2} - \varepsilon \frac{\partial T}{\partial y} \frac{\partial u}{\partial y} - \frac{\partial p}{\partial x} = 0,$$

$$(4.2) \quad (1 - \varepsilon_1 T) \frac{\partial^2 T}{\partial y^2} + \varepsilon_1 \left(\frac{\partial T}{\partial y} \right)^2 = 0.$$

The pressure gradient term $\partial p/\partial x$ in Eq. (4.1) is a known constant and thus, we do not need any algorithm to compute the pressure by imposing the incompressibility condition. The first- and second-order derivatives are discretized utilizing the standard central finite difference schemes.

The finite difference approximations are substituted in the nonlinear equations (4.1) and (4.2). The resulting difference equations are solved by using a pseudo time stepping method. An explicit Euler time integrator is employed for this purpose. The time stepping was being performed until the steady state was reached.

5. Results and discussion

Equations for ε^0 , ε^1 and ε^2 are analytically solved and their solutions are plotted for the prescribed boundary conditions. The values of used parameters in the presented work are collected in Table 1.

Table 1. Numerical values of material properties [27].

Properties	$\lambda_0 \left(\frac{\text{W}}{\text{m}\cdot\text{K}}\right)$	$\lambda_1 \left(\frac{\text{W}}{\text{m}\cdot\text{K}^2}\right)$	$\mu_0 \left(\frac{\text{N}\cdot\text{s}}{\text{m}^2}\right)$	$\mu_1 \left(\frac{\text{N}\cdot\text{s}}{\text{K}\cdot\text{m}^2}\right)$
Value	5.039×10^{-1}	5.254×10^{-3}	1.6099×10^{-3}	3.04×10^{-5}

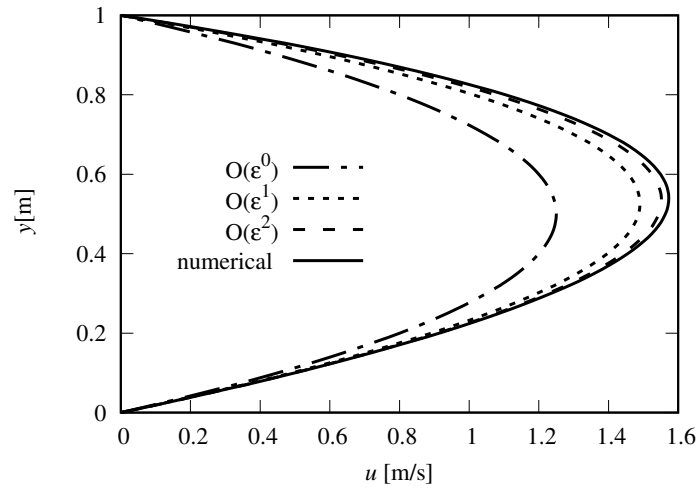


FIG. 1. Analytical and numerical solution of the velocity field at $T_d = 20^\circ\text{C}$.

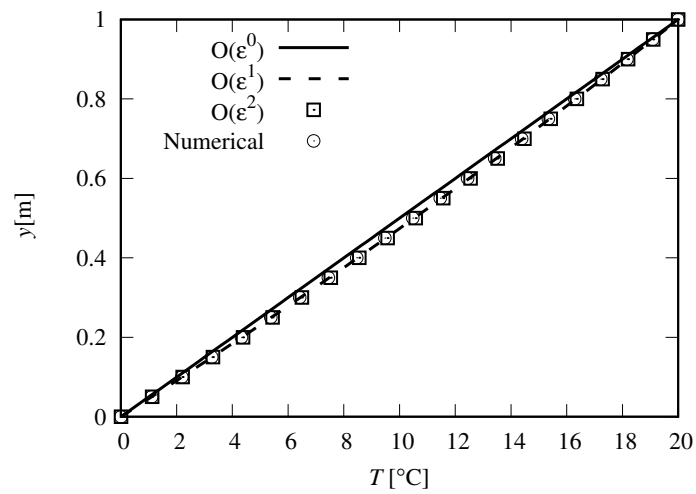


FIG. 2. Analytical and numerical solution of the temperature field at $T_d = 20^\circ\text{C}$.

For the purpose of validation, the numerical solution of the full nonlinear equations for the velocity and temperature fields is also reported. The numerical results are obtained by a finite difference discretization of the governing equations using second-order central difference schemes and solved by a pseudo-time iterative method. The domain length is 1.0 and 200 grid points are used for the discretization. The grid independency of the results is checked. As a general trend, it can be seen that the determined velocity and temperature profiles by

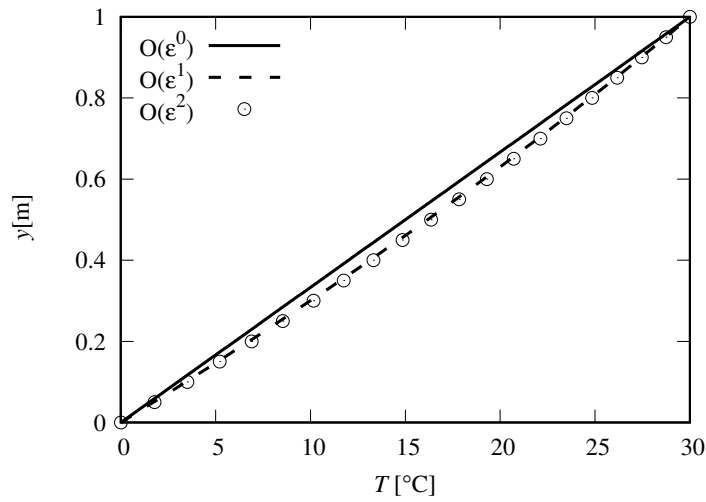


FIG. 3. Temperature field at $T_d = 30^\circ\text{C}$ obtained by different orders of approximation.

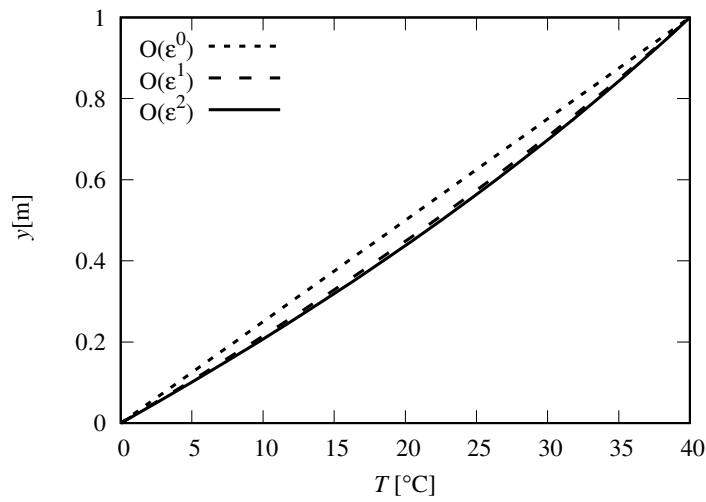


FIG. 4. Temperature field at $T_d = 40^\circ\text{C}$ obtained by different orders of approximation.

the perturbation expansion method is approaching the numerical solution by increasing the order of approximation, this is shown in Fig. 1 and Fig. 2. In Figs. 3, 4 and 5, the temperature field at $T_d = 30^\circ\text{C}$, $T_d = 40^\circ\text{C}$ and $T_d = 50^\circ\text{C}$ for different order of approximation in respect of the channel height is depicted respectively, obviously an increase in the upper wall temperature T_d makes a difference in the responses obtained by ε^0 , ε^1 and ε^2 .

Physically speaking, it is evident that with increasing the temperature in liquids, the viscosity decreases so that the fluid elements adjacent to the high-

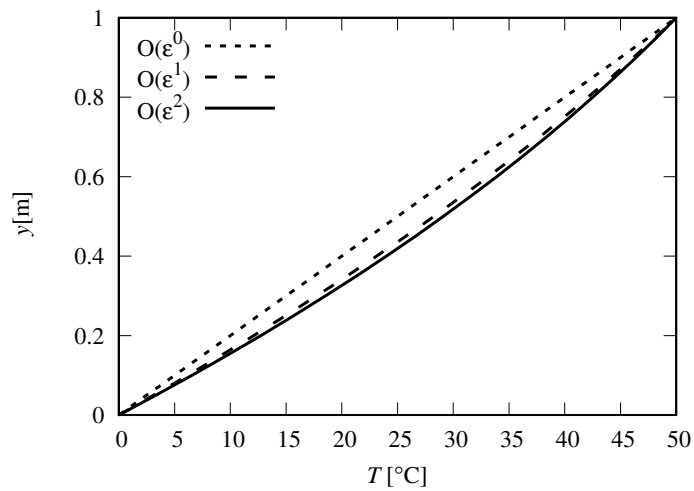


FIG. 5. Temperature field at $T_d = 50^\circ\text{C}$ obtained by different orders of approximation.

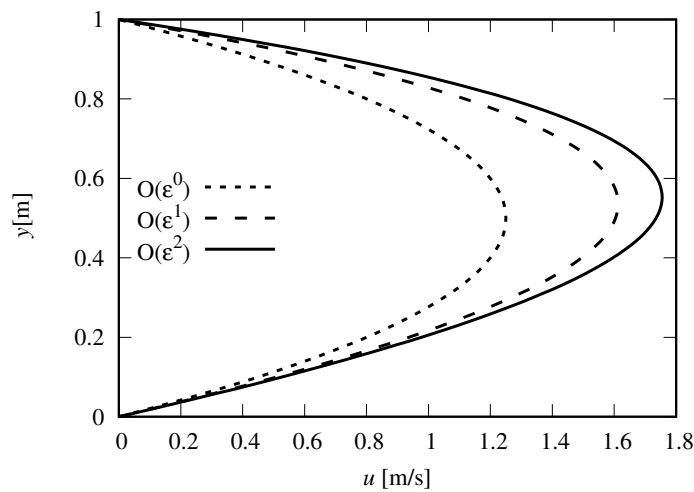


FIG. 6. Velocity field at $T_d = 30^\circ\text{C}$ obtained by different orders of approximation.

temperature wall are moving faster than those adjacent to the low-temperature wall. In this work, the effect of temperature on the viscosity is considered, thus, it is expected that the symmetry of the velocity profile is altered and the location of the maximum velocity moves from the channel center towards the high-temperature wall. Additionally, the mass flow rate (\dot{m}) throughout the channel is increased, as compared to the case of isothermal walls at the lower temperature. Figures 6, 7 and 8 show the velocity field at $T_d = 30^\circ\text{C}$, $T_d = 40^\circ\text{C}$

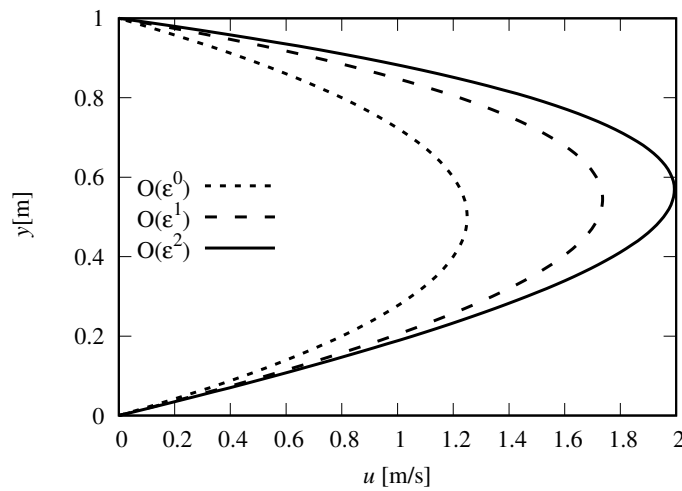


FIG. 7. Velocity field at $T_d = 40^\circ\text{C}$ obtained by different orders of approximation.

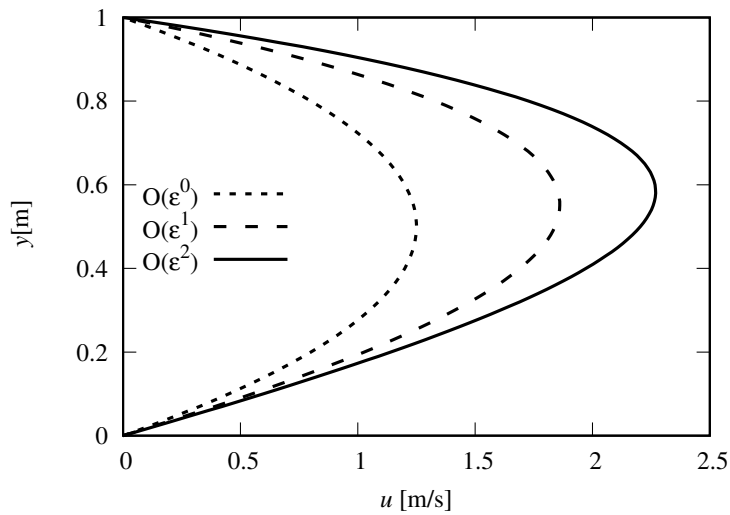


FIG. 8. Velocity field at $T_d = 50^\circ\text{C}$ obtained by different orders of approximation.

and $T_d = 50^\circ\text{C}$ for different order approximation and proves the aforementioned sentences. Figure 9 depicts the velocity field at different temperatures T_d only for second-order solution (ε^2). By increasing the temperature the velocity also increases, as mentioned above the maximum velocity moves towards the upper wall which has the highest temperature. Figures 10–14 show the shear stress at different temperatures of the upper wall and different ε . As it can be seen the shear stress profile is deviated from a linear form to a curved one, as well as the critical point of shear stress tends to move towards the high-temperature wall T_d .

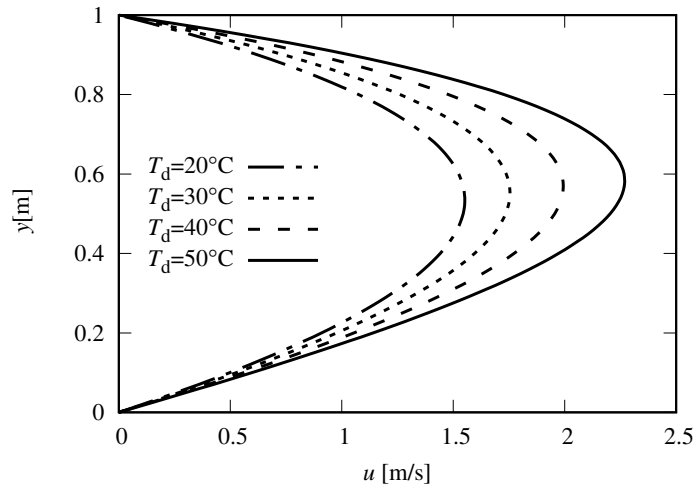


FIG. 9. Velocity field at different temperatures for $O(\varepsilon^2)$.

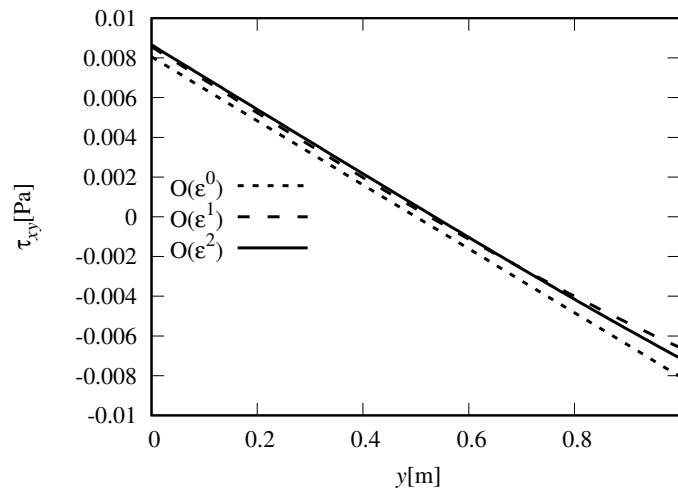


FIG. 10. Shear stress (τ_{xy}) at $T_d = 20^\circ\text{C}$ obtained by different orders of approximation.

Figure 15 is plotted to show the effect of increasing the upper wall temperature on the maximum velocity, it can be seen that with increasing the upper wall temperature the maximum velocity increases.

With improving the expansion series in the perturbation technique this agreement will also be enhanced. The velocity and temperature expansion series can be truncated after more terms to increase the accuracy of the solution.

Figure 16 shows the location of the maximum velocity as a function of the upper wall temperature for different orders of approximation. As it is expected,

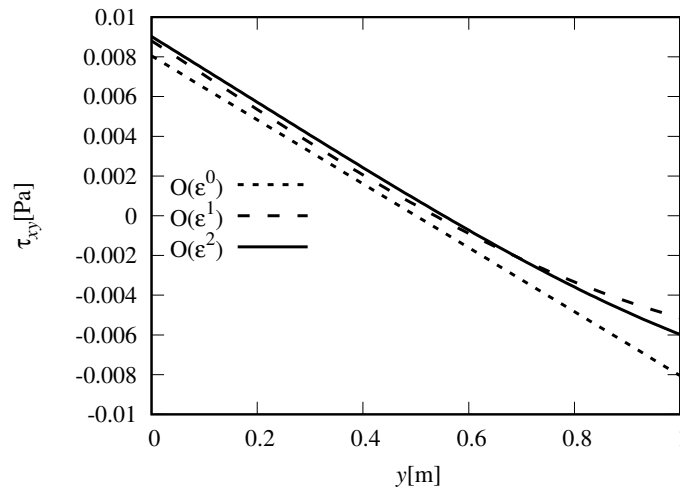


FIG. 11. Shear stress (τ_{xy}) at $T_d = 30^\circ\text{C}$ obtained by different orders of approximation.

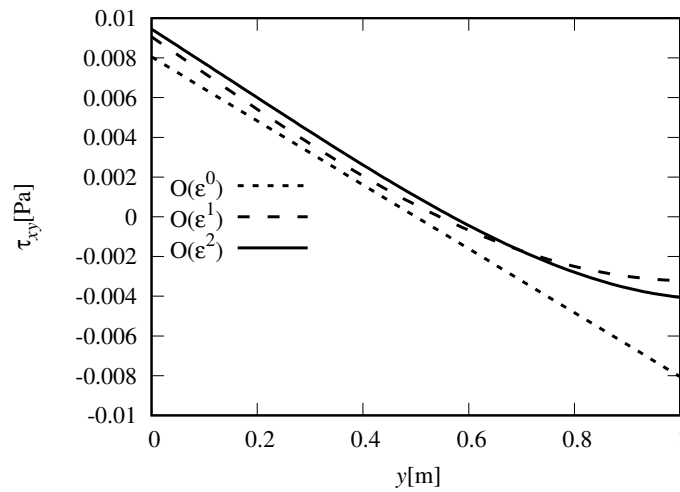


FIG. 12. Shear stress (τ_{xy}) at $T_d = 40^\circ\text{C}$ obtained by different orders of approximation.

for the linear solution $O(\varepsilon^0)$, the location at which the maximum velocity occurs is located at $0.5h$. This pertains to the case with no temperature dependence of the fluid properties. However, by the introduction of the nonlinearity, the situation differs and the location of the maximum velocity changes by changing the upper-wall temperature. The $O(\varepsilon^1)$ solution underpredicts $y(u_{\max})$ as compared to the $O(\varepsilon^2)$ solution. In any case, we have $y(u_{\max}) = 0.5h$ for the vanishing temperature difference, which is expected.

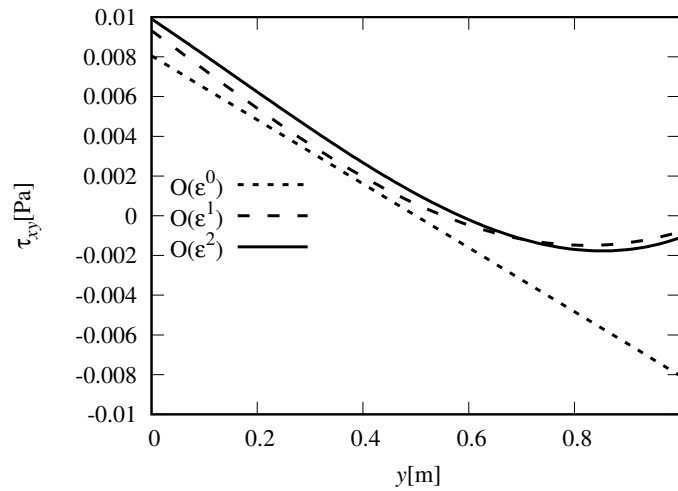


FIG. 13. Shear stress (τ_{xy}) at $T_d = 50^\circ\text{C}$ obtained by different orders of approximation.

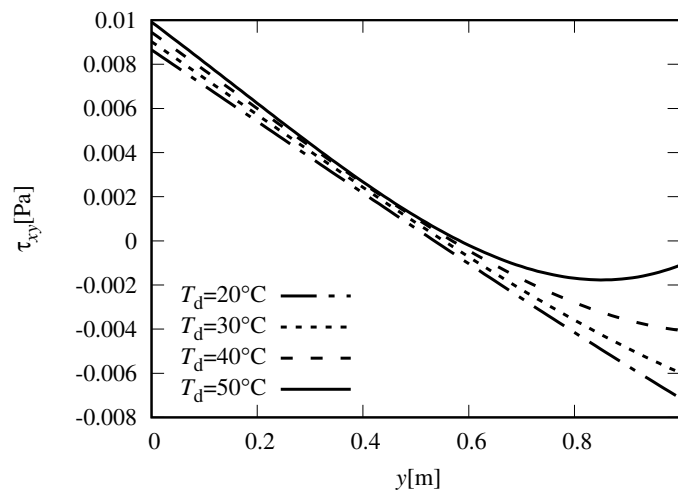


FIG. 14. Shear stress (τ_{xy}) at different temperature for $O(\varepsilon^2)$.

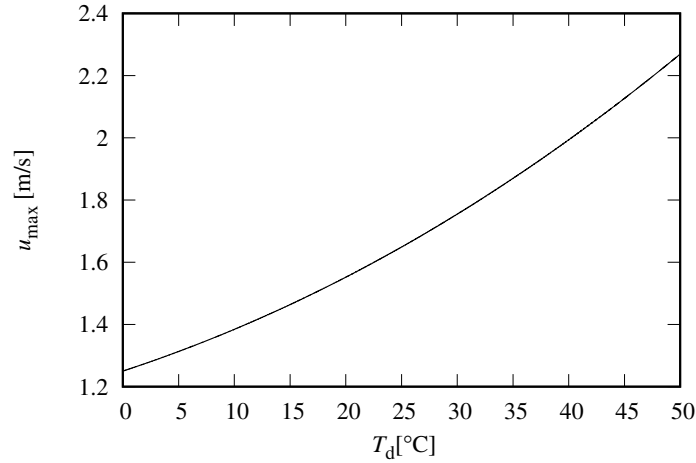


FIG. 15. Maximum velocity with respect to the upper wall temperature.

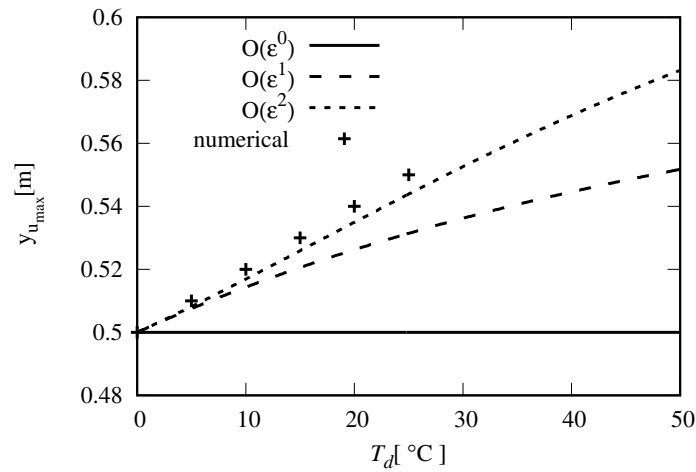


FIG. 16. Variation of the wall-normal location of maximum velocity ($y_{u_{\max}}$) with respect to the upper-wall temperature obtained from different orders of approximation and a numerical solution of the full nonlinear equation.

6. Conclusions

In this paper, a general form of using the perturbation expansion technique is presented, the proposed form is independent of any system of coordinates. The effect of the temperature-dependent viscosity and thermal conductivity on the

velocity and temperature profiles in a steady two-dimensional Couette-Poiseuille flow is analytically investigated and validated against the numerical solution. The variations of viscosity and thermal conductivity with temperature are considered to be linear functions. Increasing the order of ε for the perturbation expansion series leads to more accurate predictions for the temperature and velocity fields. Results show the maximum value of velocity in the channel is moving from the center for the $O(\varepsilon^0)$ solution towards the high-temperature wall for the higher order of ε . The analytical solution of the shear stress for the different orders of ε at different temperatures of the upper wall is determined. It is clear from the results when the temperature of the upper wall increases the critical point of the shear stress transfers towards the high temperature wall, this is for the reduction in viscosity.

We gave a general formulation of the perturbation method for the fully coupled problem. Though, its solution for all problems would not be an easy task to do. However, any problem for which a solution of momentum and energy equations exist for the constant properties case, this solution can be taken as the zeroth-order solution and higher-order approximations can be made based on that.

References

1. A.H. NAYFEH, *Perturbation Methods*, Wiley, New Jersey, 2004.
2. M. VAN DYKE, *Perturbation Methods in Fluid Mechanics*, The Parabolic Press, Stanford, 1975.
3. R.E. O'MALLEY JR., *Singular perturbation theory: a viscous flow out of Göttingen*, Annual Review of Fluid Mechanics, **42**, 1–17, 2010.
4. B.C. SAKIADIS, *Boundary layer behavior on continuous solid surface*, American Institute of Chemical Engineers, **7**, 26–28, 1961.
5. L.J. CRANE, *Flow past a stretching sheet*, Zeitschrift für angewandte Mathematik und Physik, **21**, 645–647, 1970.
6. N.G. KAFOUSSIAS, E.W. WILLIAMS, *The effect of temperature-dependent viscosity on free-forced convective laminar boundary layer flow past a vertical isothermal flat plate*, Acta Mechanica, **110**, 123–137, 1995.
7. M. XENOS, *Radiation effects on flow past a stretching plate with temperature-dependent viscosity*, Applied Mathematics, **4**, 1–5, 2013.
8. E.M.A. ELBASHBESHY, M.A.A. BAZID, *The effect of temperature-dependent viscosity on heat transfer over a continuous moving surface*, Journal of Physics D: Applied Physics, **33**, 2716–2721, 2000.
9. D. PAL, H. MONDAL, *Effect of variable viscosity on MHD non-Darcy mixed convective heat transfer over a stretching sheet embedded in a porous medium with non-uniform heat source/sink*, Communications in Nonlinear Science and Numerical Simulation, **15**, 1553–1564, 2010.

10. S.H. EMERMAN, D.L. TURCOTTE, *Stagnation flow with a temperature-dependent viscosity*, Journal of Fluid Mechanics, **127**, 507–517, 1983.
11. J.R.A. PEARSON, *Variable-viscosity flows in channels with high heat generation*, Journal of Fluid Mechanics, **83**, 191–206, 1977.
12. Y. KHAN, Q. WU, N. FARAZ, A. YILDIRIM, *The effects of variable viscosity and thermal conductivity on a thin film flow over a shrinking/stretching sheet*, Computers and Mathematics with Applications, **61**, 3391–3399, 2011.
13. J.R. BOOKER, *Thermal convection with strongly temperature-dependent viscosity*, Journal of Fluid Mechanics, **76**, 741–754, 1976.
14. S.D. GIUDICE, C. NONINO, S. SAVINO, *Effects of viscous dissipation and temperature-dependent viscosity in thermally and simultaneously developing laminar flows in microchannels*, International Journal of Heat and Fluid Flow, **28**, 15–27, 2007.
15. M.A. HOSSAIN, M.S. MUNIR, D.A.S. REES, *Flow of viscous incompressible fluid with temperature-dependent viscosity and thermal conductivity past a permeable wedge with uniform surface heat flux*, International Journal of Thermal Sciences, **39**, 635–644, 2000.
16. H.A. ATTIA, *Influence of temperature dependent viscosity on the MHD-channel flow of dusty fluid with heat transfer*, Acta Mechanica, **151**, 89–101, 2001.
17. W. YUAN, A.C. HANSEN, Q. ZHANG, *Predicting the temperature dependent viscosity of biodiesel fuels*, Fuel, **88**, 1120–1126, 2009.
18. J.M. AVELLANEDA, F. BATAILLE, A. TOUTANT, *DNS of turbulent low Mach channel flow under asymmetric high temperature gradient: Effect of thermal boundary condition on turbulence statistics*, International Journal of Heat and Fluid Flow, **77**, 40–47, 2019.
19. W. SUTHERLAND, *The viscosity of gases and molecular force*, Philosophical Magazine Series 5, **36**, 223, 507–531, 2009.
20. R. ELLAHI, *The effects of MHD and temperature dependent viscosity on the flow of non-Newtonian nanofluid in a pipe: Analytical solutions*, Applied Mathematical Modelling, **37**, 1451–1467, 2013.
21. **L. Vergori**, *Flows at small Reynolds and Froude numbers*, International Journal of Engineering Science, **48**, 1659–1670, 2010.
22. T.C. CHAIM, *Heat transfer in a fluid with variable conductivity over a linearly stretching sheet*, Acta Mechanica, **129**, 63–72, 1998.
23. CH.R. LIN, CH.K. CHEN, *Effect of temperature dependent viscosity on the flow and heat transfer over an accelerating surface*, Journal of Physics D: Applied Physics, **27**, 29–36, 1994.
24. M. DEGHAN, M.S. VALIPOUR, S. SAEDODIN, *Temperature-dependent conductivity in forced convection of heat exchangers filled with porous media: A perturbation solution*, Energy Conversion and Management, **91**, 259–266, 2015.
25. A. MOOSAIE, *A nonlinear analysis of thermal stresses in an incompressible functionally graded hollow cylinder with temperature-dependent material properties*, European Journal of Mechanics A/Solids, **55**, 212–220, 2016.
26. A. MOOSAIE, H. PANAHI-KALUS, *Thermal stresses in an incompressible FGM spherical shell with temperature-dependent material properties*, Thin-Walled Structures, **120**, 215–224, 2017.

27. R.C. REID, J.M. PRAUSNITZ, B.E. POLING, *The Properties of Gases and Liquids*, 4th ed., McGraw-Hill, New York, 1987.

Received July 22, 2020; revised version November 16, 2020.

Published online December 17, 2020.
